NUCLEAR TECHNOLOGY
EXPERIMENT

DESIGN OF A MULTICATODE COUNTER FOR SEARCHING FOR DARK PHOTONS

© 2025 A. V. Kopylov*, I. V. Orekhov, V. V. Petukhov, A. E. Solomatin

[a]Institute for Nuclear Research of the Russian Academy of Sciences Russia, Moscow

**e-mail:*kopylov@inr.ru

Received July 22, 2024

Revised August 19, 2024

Accepted September 25, 2024

Abstract. The multicathode counter is designed to search for cold dark matter, presumably consisting of hidden photons, by detecting single electrons emitted from the surface of the counter's metal cathode as a result of the conversion of hidden photons on its surface. The design of the counter allows for efficient separation of the background from ambient radioactivity and from thermal emission.electrons from the surface of the cathode filaments by subtracting the count rate measured in the gate configurationpotential. A detailed description of the design of a multi-cathode counter is given.

DOI: 10.31857/S00328162250112e8

1. INTRODUCTION

The nature of dark matter is an intriguing mystery of our time. The intrigue is that by mass it is the main component of matter filling the Universe, its mass is approximately five times greater than the mass of visible matter, but despite this, it is still not clear what dark matter consists of. Significant experimental efforts have been made to reveal the nature of dark matter, installations with a mass of several tons have been created, but the answer to this question has not yet been received. In this regard, it is proposed to expand the geography of the search, including by including in the program the search for new particles, for example, hidden photons, proposed back in the 80s of the last century [1-3]. To search for dark photons, we proposed to use the method of registering single electrons emitted from the surface of the metal cathode of a proportional counter during the conversion of a hidden photon with an energy (mass) greater than the work function of electrons from the metal, which for most metals is approximately 4 eV. In this case, dark photons themselves are considered in a number of works [4, 5] as tubular structures with an electric and magnetic field of complex configuration. To register single electrons emitted from the metal surface during the conversion of dark photons, we have developed a special design of a gas proportional counter with three cathodes. The method we propose has high sensitivity for the mass of hidden photons from 10 to 40 eV. Here we provide a detailed description of this design of a multi-cathode counter and summarize the experience we have gained over the past 8 years of research conducted using this counter.

According to [6], if dark matter consists of hidden photons, the power absorbed by the cathode during the conversion of hidden photons is described by the expression

$$P = 2\alpha^2\chi^2\rho_{CDM}A_{cath} \; . \tag{1}$$

Here $\alpha^2 = \cos^2\theta$, where θ is the angle between the electric field vector **E** of the hidden photon and the normal to the surface; $\alpha^2 = 2/3$, if the propagation direction is isotropic; χ is the kinetic mixing constant, the square of this value determines the amount of ordinary photon admixture in the hidden photon amplitude; ρ_{CDM} is the energy density of cold dark matter, which was taken here as 0.4 GeV/cm ^{3} ; A_{cath} is the cathode area. If the energy (mass) of a hidden photon exceeds the work function of electrons from the cathode metal, the conversion of the hidden photon will cause the emission of a single electron with a certain quantum efficiency η . In this case, the power absorbed by the cathode can be found from the count rate of single electrons emitted by the cathode:

$$P = m_{\gamma'} R_{MCC}/\eta \; . \tag{2}$$

Here $m_{\gamma'}$ – mass (energy) of the hidden photon; R_{MCC} – single electron count rate, here it is assumed that this rate is determined exclusively by the conversion of hidden photons into a regular photon with subsequent electron emission; η – quantum efficiency for the single electron emission process, which is assumed here to be equal to the quantum efficiency for a real photon with energy $m_{\gamma'}$. Combining expressions (1) and (2), we get

$$\chi_{sens} = 2.9 \cdot 10^{-12} \left(\frac{R_{MCC}}{\eta \cdot 1\text{Гц}}\right)^{1/2} \left(\frac{m_{\gamma'}}{1\text{эВ}}\right)^{1/2} \left(\frac{0.3\text{ГэВ/см}^3}{\rho_{CDM}}\right)^{1/2} \left(\frac{1\text{м}^2}{A_{MCC}}\right)^{1/2} \left(\frac{\sqrt{2/3}}{\alpha}\right) . \tag{3}$$

It follows from this expression that the main limitation of the method is the background count rate of single electrons, which for standard photon detectors such as PMT, VEU, photon counters based on gas electron multipliers constitutes a rather significant value, about 10^{-1} Hz/cm ^{2} and higher. In the method we developed for measurements using a special detector – a multicathode counter – the background count rate of single electrons according to the results of our measurements [7–9] was less than 10^{-4} Hz/cm ^{2} for a counter with a copper cathode and less than 10^{-5} Hz/cm ^{2} for a counter with an aluminum cathode. Since the quantum efficiency of the metals we use for the solid cathode of the counter is maximal in the range from 10 to 40 eV, our proposed method for searching for dark photons has the highest sensitivity for hidden photon masses in this range. The calculated density of dark photon particles is from 10 to 40 million particles per cubic centimeter, based on our accepted value of $\rho_{CDM} = 0.4$ GeV/cm ^{3}. For comparison, the density of relic neutrinos and the density of relic photons are approximately 150 n and 500 particles per cubic centimeter, respectively.

2. CONSTRUCTION OF THE MULTI-CATHODE COUNTER

Figure 1 shows a multi-cathode counter. The design was based on a gas-filled proportional counter. Mixtures of Ar + 10% CH_4 and Ne + 10% CH_4 were used as the working gas. Unlike a conventional proportional counter, it has not one but three cathodes. The schematic diagram of the multi-cathode counter was presented by us in paper [7]. Upper limits on the kinetic mixing constant for dark photon masses from 10 to 40 eV were obtained [8]. Here we provide a more detailed description of the device, based on our operational experience and the results of our research. The outer cathode *4* in the form of a solid metal cylinder is a source of single electrons, which are presumably emitted from the cathode surface during the conversion of hidden photons. As follows from expression (3), the larger the surface of this cathode, the higher the sensitivity of the detector. In different counters, we used a metal cathode with a diameter ranging from 140 to 200 mm and a length of approximately 500 mm, with the cathode area ranging from 0.2 m ^{2} to 0.3 m^2.

Fig. 1. Image of the multi-cathode counter.

Electrons emitted from the outer cathode drift toward the central counter, where they form electron avalanches near the anode surface *5*. The anode is made of a gold-plated tungsten-rhenium alloy wire with a diameter of 25 μm. To register single electrons, a large gas amplification coefficient (more than 10^5) is required, and consequently, a large field gradient near the anode. To provide the required field gradient, the first cathode *6* of the central counter has a relatively small diameter (about 40 mm). This cathode is made of nichrome wires with a diameter of 50 μm, stretched at a distance of approximately 6.5 mm from each other in a circle around the anode. At a distance of about 5 mm from the outer cathode is the second cathode *7*, also made of nichrome wires with a diameter of 50 μm, stretched at a distance of about 4.8 mm from each other in a circle near the outer cathode. The distance between the wires was chosen mainly for technological reasons. The counter calibration results showed that the field inhomogeneity did not significantly affect the detector characteristics. A view of the internal elements of the counter from the end is shown in Fig. 2.

Fig. 2. View of the internal elements of the counter from the end.

The assembly of the counter was a non-trivial task, mainly due to the complexity of the multi-cathode design. To tension the coaxial system of wire electrodes (threads), special equipment with three guide rods was used, as shown in Fig. 3. After tensioning the wires, the entire system was placed inside the outer metal cathode, the end insulating discs made of acrylic glass were fixed to the ends of the metal cathode, and the guide rods were removed. To reduce the edge effect, ring-shaped focusing electrodes were placed on the inner side of the acrylic discs, to which the potential of the second cathode was applied.

Fig. 3. Multi-cathode system with equipment.

The counter operates in two configurations that differ in the potential difference between the second and outer cathodes, as shown in Fig. 4.

Fig. 4. Potentials in configurations 1 and 2.

In configuration 1, the potential on the outer cathode is lower than the potential on the second cathode by approximately 20 V, so that electrons emitted from the surface of the outer cathode can freely drift towards the central counter. In this configuration, the effect plus background is measured. The effect is determined by the rate of single electron emission from the surface of the outer metal cathode. The background is determined by two processes: emission from the surface of the wires and events from ionizing particles crossing the counter along short tracks at both of its ends.

In configuration 2, the potential on the second cathode is lower than the potential on the outer cathode by approximately 40 V. In this configuration, electrons emitted from the surface of the outer cathode cannot drift to the central counter, since the second cathode serves as a barrier here, on which electrons are scattered back toward the outer cathode. In this configuration, the counter measures only the background due to the latter two channels.

To determine the optimal potential difference between the second and outer cathodes in configurations 1 and 2, measurements of the counting rate were performed when the counter was irradiated with UV radiation from a mercury lamp, the results of which are presented in Fig. 5, taken from work [9]. As follows from this figure, the optimal potential difference is +20 V for configuration 1 and –40 V for configuration 2. With a potential difference of more than +20 V, part of the electrons emitted from the outer cathode is captured by the second cathode, which leads to the loss of some events. The potential difference of –40 V for configuration 2 was chosen as a value that reliably ensures complete suppression of events from electrons from the outer cathode in this configuration. It should be noted that this potential difference is much less than the values of the potentials themselves, which are approximately 2300 V, and therefore it can be expected that a small change in the potential on the outer cathode when switching from one configuration to another does not affect the counting characteristic of the counter. This was confirmed by the results obtained during the calibration of the counter.

Fig. 5. Counting rate during counter calibration as a function of the potential difference between the first and second cathodes $\Delta U = U_2 - U_1$.

The effect is calculated as the difference in counting rate between two configurations $R_1 - R_2$. We do not know the proportion of each of these two channels in background generation. This uncertainty is the main source of systematic measurement error. Indeed, when subtracting the background due to electrons emitted from the surface of the second cathode wires, it should be taken into account that electrons emitted toward the outer cathode will not reach the central counter, as they will be trapped in the space between the outer and second cathodes. The background magnitude depends on the material from which the cathode wires are made. If we consider both background channels: from electrons emitted from the wire surface (*a*) and from the edge effect (*b*), we get a system of two equations for two different configurations of the multi-cathode counter:

$$a + b = R_1 \qquad (4)$$

for the first configuration and

$$a + kb = R_2 \qquad (5)$$

for the second configuration. Here $k = (n_1 + n_2/2)/(n_1 + n_2)$, where n_1 and n_2 are the number of wires in the first and second cathodes respectively. Solving this system of equations, we find

$$b = (R_1 - R_2)/(1 - k) \qquad (6)$$

and, accordingly,

$$a = R_1 - b. \qquad (7)$$

To achieve high measurement sensitivity, it is necessary that the wire contribution to the background is negligibly small. When this condition is met, the background in the first and second configurations will be approximately equal, and the procedure for subtracting the background measured in the second configuration from the total counting rate measured in the first configuration will be correct. Thus, it is necessary to select such a material for the counter wires that would give a negligibly small background from the wires. For this purpose, we conducted measurements of the counting rate with counters of identical design but with wires made of different materials. In the first case, we used nichrome wires, and in the second case, gold-plated tungsten-rhenium alloy wires. In both cases, the wire thickness was 50 microns.

Figure 6 shows the results of measurements over 100 days on a counter with nichrome wires. This figure shows that the average counting rates in the first and second configurations were approximately equal and, consequently, the contribution of the wires to the background was negligibly small. Figure 7 shows the results of measurements over 40 days on a counter with tungsten-rhenium alloy wires. The average counting rates in the two configurations differed significantly in this case. In this counter design the number of wires was: $n_1 = 20$, $n_2 = 100$ and $k = 0.58$. Hence, following expressions (6) and (7), we find $b = 0.17$ Hz and $a = 0.10$ Hz.

Fig. 6. Counting rates measured on a counter with nichrome wires – bottom figure, counter temperature – top figure.

Fig. 7. Counting rates measured on a counter with gold-plated tungsten-rhenium alloy wires.

The total length of wires of the first and second cathodes in both cases was 60 meters. Thus, the electron emission rate from the surface of the gold-plated tungsten-rhenium alloy wire was $2.8 \cdot 10^{-3}$ Hz per meter of wire. The relatively high emission rate can be explained by the presence of long-lived ($T_{½} = 4.1 \cdot 10^{10}$ years) radioactive isotope ^{187}Re in rhenium, the content of which in natural rhenium is 62.6%. As a possible mechanism, we can assume the saturation of metastable levels of metallic tungsten by beta particles from the decay of ^{187}Re, the de-excitation of which leads to the emission of electrons from the surface of the wires. Based on the results of these measurements, we see that nichrome is a more suitable material for cathodes of a multi-cathode counter.

During exposure, the counter was placed in a special steel box with a wall thickness of approximately 300 mm to suppress external gamma radiation. The 300 mm steel shielding provides attenuation of the 1460.7 keV line from ^{40}K by approximately $5 \cdot 10^3$ times, the 1764.5 keV line from ^{214}Bi by approximately $3 \cdot 10^3$ times, and the 2614.5 keV line from ^{208}Tl by approximately 10^3 times. However, the effective attenuation coefficient of the background from external gamma radiation is much lower. The background is determined mainly by the intensity near the maximum of the gamma radiation spectrum at energies from approximately 100 to 200 keV. We measured the gamma radiation spectrum outside and inside the passive shielding using a low-background NaI(Tl) detector, and based on the measurement results, we found that in this energy range, the gamma radiation intensity was attenuated by the shielding by approximately 100 times. For the counter with a copper cathode, the measured count rate of single electrons outside the passive shielding was about 20% higher than the rate inside the shielding. This shows that the contribution of external gamma radiation to the single electron count rate for this counter was negligibly small, less than 0.2%. Further improvement of the detector using purer materials, as we hope, will allow achieving a lower background count rate. In this case, the background contribution from external gamma radiation can no longer be neglected. Additional passive shielding made of material with lower uranium, radium, and thorium content may also be required. These issues are subject to further research.

3. CONCLUSION

The design of a multicathode counter is described. The counter is used to search for dark photons by registering single electrons emitted from the surface of a solid metal cathode during the conversion of dark photons on its surface [10]. The counter has the highest sensitivity for a dark photon mass of 10 to 40 eV. The calculated density of hidden photons with such masses is from 10 to 40 million particles per cubic centimeter, if we take the density of dark matter in the vicinity of the Sun to be approximately 0.4 GeV per cubic centimeter. For comparison, the density of relic neutrinos is approximately 150 particles per cubic centimeter, and the density of relic photons is approximately 500 particles per cubic centimeter. The background count rate of the multicathode counter depends on the material of the cathode filaments. The emission rate of single electrons from the surface of nichrome filaments and from a gold-plated tungsten-rhenium alloy was measured. It is shown that the use of nichrome provides a lower background of the multi-cathode counter. This result can be used in the design of multi-wire gas detectors of ionizing radiation.

FUNDING

The work was carried out with the support of the Ministry of Science and Higher Education within the framework of the federal project “Development of infrastructure for scientific research and personnel training” of the state project “Science and Universities” dated December 28, 2023 No. DS/45-pr.

REFERENCES

1. *Fayet P.*// Nucl. Phys. 1981. V. 187. P. 184. https://doi.org/10.1016/0550-3213(81)90122-X
2. *Okun L.B.*// Sov. Phys. JETP. 1982. V. 56. P. 502.
3. *Georgi H., Ginsparg P.H., Glashow S.L.*// Nature. 1983. V. 306. P. 765. https://doi.org/10.1038/306765a0

4. *Dzunushaliev V., Folomeev V.*// Phys. Rev. D. 2021. V. 104. P. 116027. https://doi.org/10.1103/PhysRevD.104.116027
5. *Dzunushaliev V., Folomeev V.*// Phys. Rev. D. 2022. V. 105. P. 016022.https://doi.org/10.1103/PhysRevD.105.016022
6. *Horns D., Jackel J., Lindner A., Lobanov A., Redondo J., Ringwald A.*// J. Cosmol. Astropart. Phys. 2013. V. 4. P. 16.https://doi.org/10.1088/1475-7516/2013/04/016
7. *Kopylov A., Orekhov I., Petukhov V.*// Nucl. Instrum. Methods. Phys. Res. A. 2018. V. 910. P. 164.https://doi.org/10.1016/j.nima.2018.09.075
8. *Kopylov A., Orekhov I., Petukhov V.* // J. Cosmol. Astropart. Phys. 2019. V. 07. P. 008. https://doi.org/10.1088/1475-7516/2019/07/008
9. *Kopylov A.V., Orekhov I.V., Petukhov V.V.* // Physics of Atomic Nuclei. 2019. V. 82. P. 1317. https://doi.org/10.1134/S1063778819090060
10. *Kopylov A., Orekhov I., Petukhov V.* // Moscow University Physics Bulletin. 2022. V. 77. P. 315. https://doi.org/10.3103/S002713492202053

FIGURE CAPTIONS

Fig. 1. Image of the multi-cathode counter: *1* – quartz glass, *2* – windows for calibration, *3* – housing, *4* – external cathode, *5* – anode, *6* – first cathode, *7* – second cathode, *8* – preamplifier.

Fig. 2. View of the internal elements of the counter from the end. Wires at small diameter – first cathode, at large diameter – second cathode.

Fig. 3. Multi-cathode system with equipment: *1* – end disks made of plexiglass (polymethyl methacrylate), *2* – focusing ring electrodes,
3 – guide rods, *4* – second cathode wires, *5* – first cathode wires, *6* – anode wire, *7* – contact pads for wires.

Fig. 4. Potentials in configurations 1 and 2.

Fig. 5. Count rate during counter calibration as a function of the potential difference between the first and second cathodes $\Delta U = U_2 - U_1$. Arrows indicate the optimal potential difference for configurations 1 and 2.

Fig. 6. Count rates measured on the counter with nichrome wires – bottom figure, counter temperature – top figure.

Fig. 7. Count rates measured on the counter with gold-plated tungsten-rhenium alloy wires. Dark points – configuration 1, light points – configuration 2.

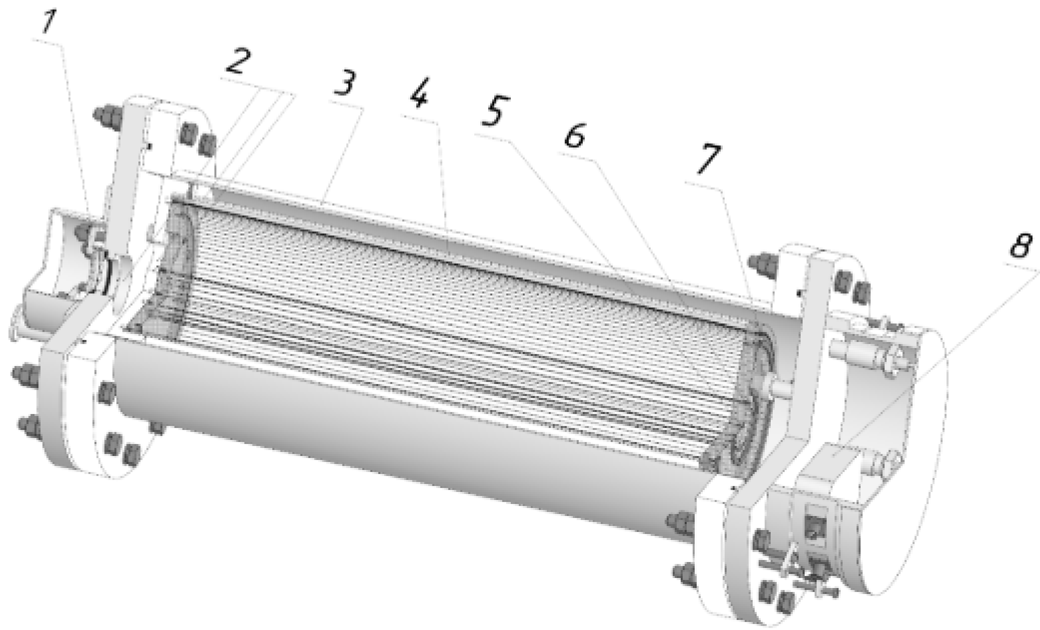

Fig. 1.

Fig. 2.

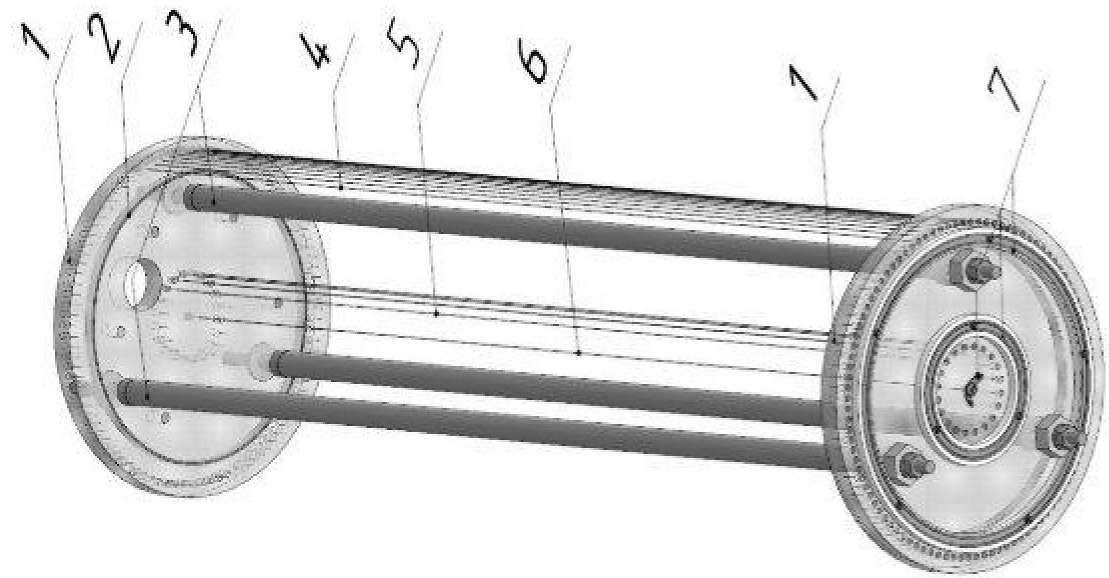

Fig. 3.

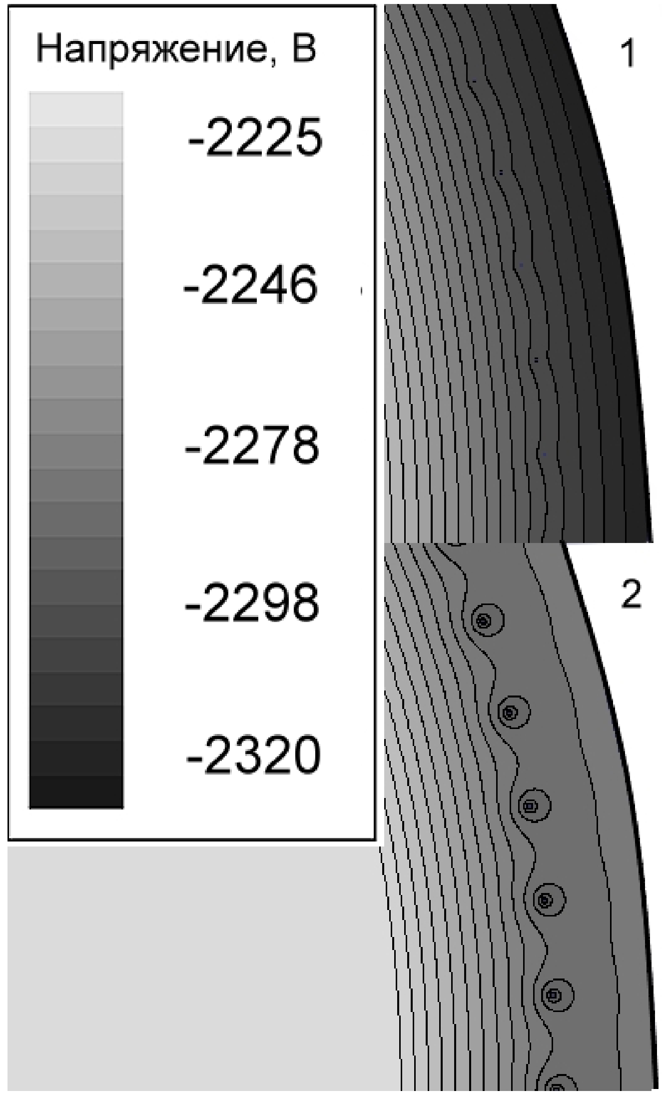

Fig. 4.

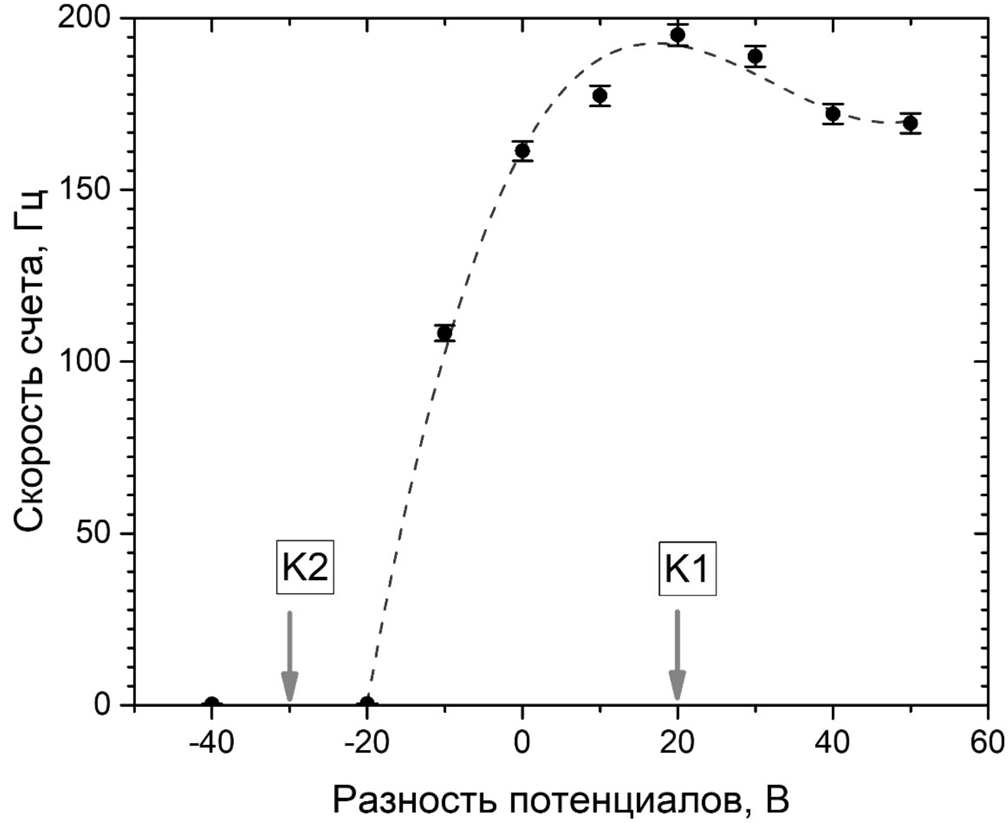

Скорость счета, Гц
200
150
100
50
0
K2
K1
-40
-20
0
20
40
60
Разность потенциалов, В

Fig. 5.

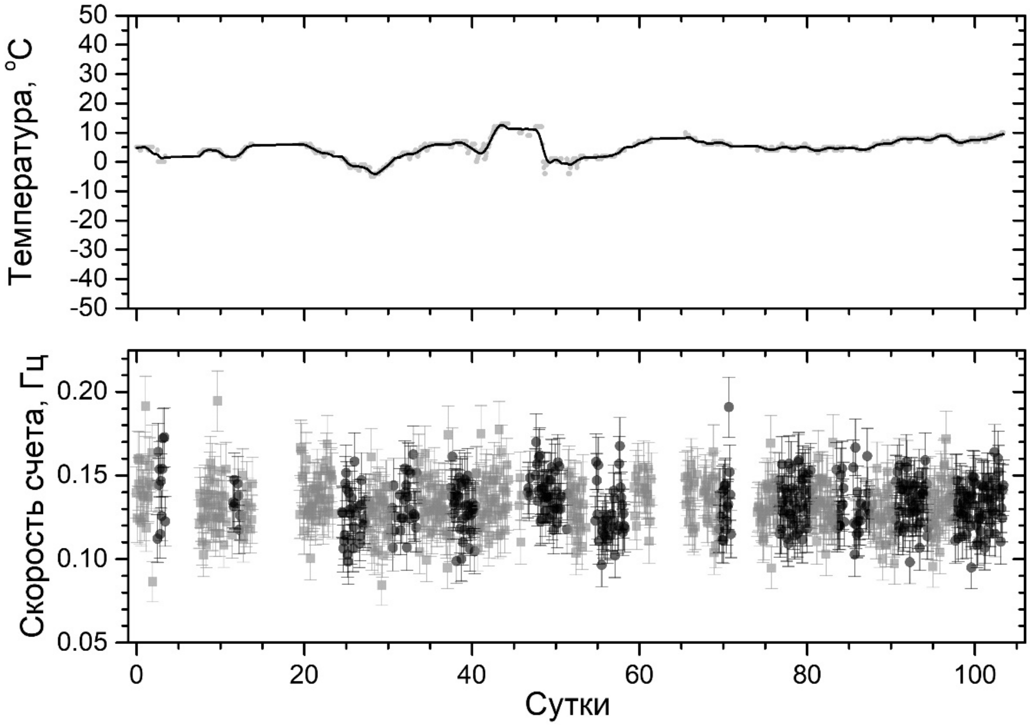

Fig. 6.

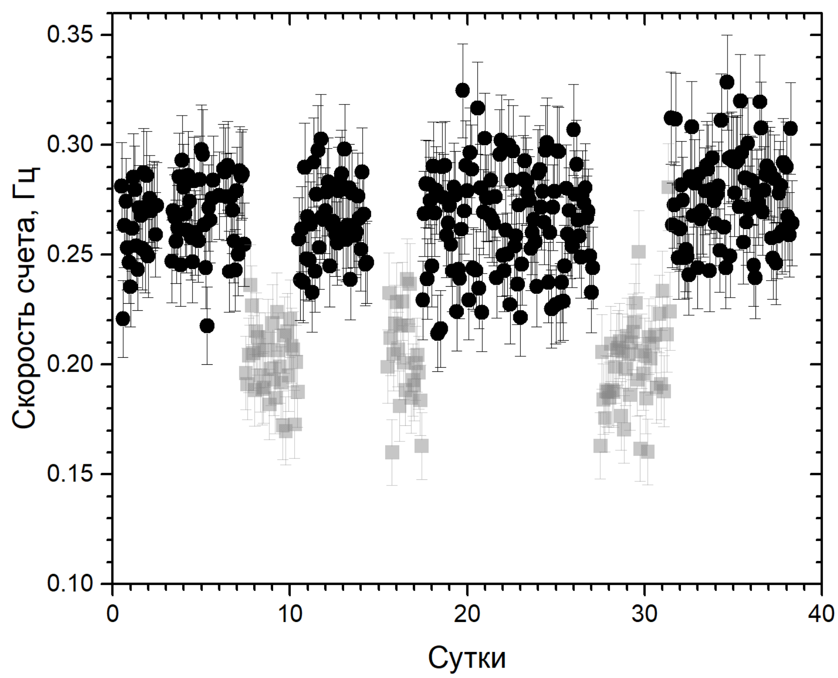

Fig. 7.